

An evaluation of total variation signal denoising methods for partial discharge signals

Mitiche, I.; Morison, G.; Nesbitt, A.; H.-Narborough, M.; Boreham, P.; Stewart, B.G.

Published in:
2017 INSUCON - 13th International Electrical Insulation Conference (INSUCON)

DOI:
[10.23919/INSUCON.2017.8097195](https://doi.org/10.23919/INSUCON.2017.8097195)

Publication date:
2017

Document Version
Peer reviewed version

[Link to publication in ResearchOnline](#)

Citation for published version (Harvard):
Mitiche, I, Morison, G, Nesbitt, A, H.-Narborough, M, Boreham, P & Stewart, BG 2017, An evaluation of total variation signal denoising methods for partial discharge signals. in *2017 INSUCON - 13th International Electrical Insulation Conference (INSUCON)*. IEEE. <https://doi.org/10.23919/INSUCON.2017.8097195>

General rights

Copyright and moral rights for the publications made accessible in the public portal are retained by the authors and/or other copyright owners and it is a condition of accessing publications that users recognise and abide by the legal requirements associated with these rights.

Take down policy

If you believe that this document breaches copyright please view our takedown policy at <https://edshare.gcu.ac.uk/id/eprint/5179> for details of how to contact us.

AN EVALUATION OF TOTAL VARIATION SIGNAL DENOISING METHODS FOR PARTIAL DISCHARGE SIGNALS

I. Mitiche*, G. Morison*, A. Nesbitt*, M. Hughes-Narborough*, P. Boreham**, and B. G. Stewart***

*Department of Engineering, Glasgow Caledonian University, United Kingdom

** Doble Engineering, United Kingdom

*** Department of Electronic and Electrical Engineering, University of Strathclyde, United Kingdom

INTRODUCTION

Partial discharge (PD) monitoring in high voltage power plants is a useful tool to detect the presence of insulation degradation in the electrical systems [1]. Specifically, condition assessment of power systems has the advantage of reducing maintenance and repair costs, downtime and reducing risks. This requires measurement of field PD signals which are often observed in an environment contaminated by Additive White Gaussian Noise (AWGN) which may mask relevant PD information [2]. The use of Electromagnetic Interference (EMI) testing has also been suggested for condition assessment of insulation systems in turbine-driven generators. These techniques allow online testing which avoids generator shutdown during long inspections [3]. Power assets such as transformers, generators and cables surround the EMI signals making them very susceptible to noise. This affects the relevant information contained in the signal which hinders the analysis for PD identification and may affect the classification accuracy of PD. The proposed solution is to employ signal denoising techniques for noise mitigation in the captured field signals. Several denoising methods have been used on PD signals. The most popular technique is wavelet-based which has successfully denoised simulated and real PD signals combined with hard and soft thresholding of the wavelet coefficients [4]. The Wavelet Transform (WT) was exploited in [5] using high spatial correlation and Support Vector Machine (SVM) methods to distinguish the relevant PD coefficients from noise. However, this method is complex for practical implementation. A similar decomposition method using the eigen approach was implemented in [6] to reduce noise collected in field PD data. Different techniques for wavelet coefficient selection were introduced for enhanced PD denoising in [7,8]. The Complex Wavelet Transform (CWT) was used instead of WT in [9,10], in combination with simple and combined information, for signal denoising because of CWT adaptivity to the non-stationary PD signal. However, PD signal denoising is still an ongoing area of research which aims to achieve improved results for non-stationary nature signals.

Ding and Selesnick introduced Wavelet TV (WATV) algorithm [11] which outperforms wavelet transform based denoising techniques. WATV employs undecimated wavelet transform combined with Total Variation (TV). The purpose in this work is to extend upon and compare against WATV algorithm by developing a method which employs the principle of signal decomposition, which is suitable for non-stationary signals such as PD signals. This is achieved using Adaptive Local Iterative Filtering (ALIF) [12] to develop a novel denoising approach named as ALIF-TV, inspired by WATV algorithm, where the denoised signal is constructed by solving a non-convex optimisation problem. The methods are applied to practical PD EMI measurements signals collected in a power plant. The following section briefly defines the noise problem in PD signals and the denoising algorithms employed in this work. Next, the EMI PD signal measurement approach is described. Denoising results are then presented in which the performance of the algorithms are compared using a Mean Square Error (MSE) approach. Finally conclusions are drawn to summarise the main findings of this work.

PROBLEM FORMULATION

We consider a signal $y(n)$ contaminated by AWGN formulated as:

$$y(n) = x(n) + \eta(n), n = 1, 2, \dots, N \quad (1)$$

where $\eta(n)$ is the Gaussian distribution random variables with noise standard deviation (σ_η) and $x(n)$ is the noise free signal. The goal is to extract an approximate signal $\hat{x}(n)$ which is as close as possible to the noise-free signal with minimum error.

TV-BASED ALGORITHMS

WATV algorithm

This technique employs the WT (W) of a signal y which has as coefficients $\omega = Wy$. The latter are indexed as $\omega_{j,k}$ where j and k represent the

indices of scale and time respectively. WATV can use any transform which satisfies the Parseval frame condition defined as:

$$W^T W = I. \quad (2)$$

Where I is the identity matrix. In this work the undecimated WT is used in WATV. Let the TV of a signal x be defined as follows:

$$TV(x) := \|Dx\|_1 \quad (3)$$

where D is the 1st order difference matrix which is defined in Equation (4) and $\|x\|_1$ is the ℓ_1 norm of a signal x , which can be calculated using Equation (5).

$$D = \begin{pmatrix} -1 & 1 & & & \\ & -1 & 1 & & \\ & & \ddots & \ddots & \\ & & & -1 & 1 \end{pmatrix} \quad (4)$$

$$\|x\|_1 = \sum_i^N |x_i|. \quad (5)$$

The WATV algorithm solves the non-convex optimisation problem, using TV, which produces noise free wavelet coefficients:

$$\hat{\omega} = \arg \min_{\omega} \left\{ F(\omega) = \frac{1}{2} \|Wy(n) - \omega\|_2^2 + \sum_{j,k} \lambda_j \phi(\omega_{j,k}; \alpha_j) + \beta \|DW^T \omega\|_1 \right\} \quad (6)$$

where $\|DW^T \omega\|_1$ represents the total variation, $\lambda_j > 0$ and $\beta > 0$ are regularisation parameters and α_j is the penalty parameter. α_j and λ_j change according to the decomposition level of the signal j .

The reconstruction of the noise free signal $\hat{x}(n)$ is obtained through the inverse WT given by:

$$\hat{x} = W^T \hat{\omega}. \quad (7)$$

This non-convex optimisation problem is solved using the Split Augmented Lagrangian Shrinkage Algorithm (SALSA) [13]. First, by employing variable splitting

to the optimisation problem in Equation (6) the expression in Equation (8) can be written as

$$\arg \min_{\omega} g_1(\omega) + g_2(u) \quad (8)$$

Subject to $u = \omega$,

Given that

$$g_1(\omega) = \frac{1}{2} \|Wy - \omega\|_2^2 + \sum_{j,k} \lambda_j \phi(\omega_{j,k}; \alpha_j) \quad (9)$$

$$g_2(u) = \beta \|DW^T \omega\|_1$$

the augmented Lagrangian is calculated as:

$$L(\omega, u, \mu) = g_1(\omega) + g_2(u) + \frac{\mu}{2} \|u - \omega - d\|_2^2 \quad (10)$$

where $\mu > 0$, $d = 0$ in the initial iteration and $\|x\|_2$ is the ℓ_2 norm of a signal x .

Equation (8) can be solved by an iterative algorithm which contains three steps:

$$\omega = \arg \min_{\omega} \left\{ g_1(\omega) + \frac{\mu}{2} \|u - d - \omega\|_2^2 \right\} \quad (11)$$

$$u = \arg \min_u \left\{ g_2(u) + \frac{\mu}{2} \|u - d - \omega\|_2^2 \right\} \quad (12)$$

$$d = d - (u - \omega) \quad (13)$$

The overall WATV algorithm with SALSA optimisation problem solving is summarised as follows in Table 1:

Table 1. WATV iterative algorithm

Inputs: y, λ_j, β, μ
Initialise: $\mu = Wy, d = 0, a_j = \frac{1}{\lambda_j}$
Repeat:
$p = (Wy + \mu(u - d)) / (\mu + 1)$
$\omega = \theta(p_{j,k}; \lambda_j / (\mu + 1), a_j)$ for all j, k
$v = d + \omega$
$u = v + W(\text{tvd}(W^T v, \beta / \mu) - W^T v)$
$d = d - (u - \omega)$
Until convergence
Return: $\hat{x} = W^T \omega$

where tvd is the total variation denoising algorithm, θ is arctangent thresholding function, and the TV regularization parameters are defined as:

$$\beta = (1-\eta)\sqrt{N}\sigma / 4 \quad (14)$$

$$\lambda = (2.5\eta\sigma) / \sqrt{2^j} \quad (15)$$

A nominal value of $\eta = 0.95$ was selected to control the weight of the TV and the wavelet components of the optimization problem in Equation (6). Since the noise variance σ within the signal is unknown, it is derived using the Donoho Median Absolute Deviation (MAD) proposed in [14] which is defined as:

$$\sigma = MAD(y) / 0.6745. \quad (16)$$

ALIF-TV algorithm

ALIF is a recursive approach that splits a multicomponent signal into a predefined number of signal components called the Intrinsic Mode Function (IMF), which are arranged in decreasing frequency order [12]. It is similar to Empirical Mode Decomposition (EMD) in structure, but ALIF theory has a mathematical framework, unlike EMD. In addition, it overcomes the mode mixing issue of EMD [15]. Let:

$$y(n) = IMF_1(n) + IMF_2(n) + \dots IMF_K(n) + R(n)$$

be the signal which is decomposed into $IMF_j(n); j = 1, 2, \dots, K$ IMFs plus a residual trend R. The filtering output of ALIF is obtained by

$$y_{j+1}(n) = y_j(n) - \sum_{m=-l_j(n)}^{l_j(n)} h_j(n, m) \cdot y_j(n+m) \quad (17)$$

where $h_j(n, m) \in \mathbb{R}$, $n \in [-l_j(n), l_j(n)]$ are the coefficients of a low pass filter at point n with length $2l_j(n) + 1$.

The algorithm uses a sequence of inner and outer iterations to obtain the IMFs plus residual. The inner one is iterated over Eq. (14) to extract the IMFs when it converges. The outer iteration converges to obtain the residual when the number of extreme points in $y_j(n)$ is constantly decreasing as the number of iterations increases i.e. when the trend signal is obtained.

The theory of ALIF is summarized in Table 2.

Let $IMF = Ay$ be the IMFs obtained using the ALIF algorithm and $A^T = \sum_{j=1}^K IMF_j$ is its

reconstruction. This algorithm replaces the undecimated WT in the WATV algorithm by ALIF thus the IMFs are thresholds instead of wavelet coefficients. The complete ALIF-TV algorithm is summarized in Table 3.

Table 2 ALIF algorithm

<p>IMF = { }</p> <p>while the number of extrema ≥ 2 do</p> <p>$y_1(n) = y(n)$</p> <p>while the stopping criteria is not satisfied do</p> <p>Calculate filter length $l_j(n)$ and filter coefficients for $f(n)$</p> $y_{j+1}(n) = y_j(n) - \sum_{m=-l_j(n)}^{l_j(n)} h_j(n, m) \cdot y_j(n+m)$ <p>$j = j + 1$</p> <p>end while</p> <p>IMF = IMF \cup $y_j(n)$</p> <p>$y(n) = y(n) - y_j(n)$</p> <p>end while</p> <p>IMF = IMF \cup $y(n)$</p>
--

Table 3 ALIF-TV algorithm

<p>Inputs: y, λ_j, β, μ</p> <p>Initialise: $\mu = Ay, d = 0, a_j = \frac{1}{\lambda_j}$</p> <p>Repeat:</p> <p>$p = (Ay + \mu(u - d)) / (\mu + 1)$</p> <p>$IMF = \theta(p_{j,k}; \lambda_j / (\mu + 1), a_j)$ for all j, k</p> <p>$v = d + \omega$</p> <p>$u = v + A(tv d(A^T v, \beta / \mu) - A^T v)$</p> <p>$d = d - (u - IMF)$</p> <p>Until convergence</p> <p>Return: $\hat{x} = W^T \omega$</p>

METHODOLOGY

Partial Discharge Data Acquisition

The PD signals used in this work were measured in a real life generator and transformer within a power plant. The data presented is from a synchronous generator and associated step-up transformer (GSU). The generator under test is a General Electric (GE), 991MVA, 26kV, hydrogen/water cooled synchronous generator manufactured in 1983. The GSU under test is a GE 968MVA, 3-phase 26kV/345kV 3-phase transformer manufactured in 1984. EMI data from both are collected from the temporary installation of a single

split core radio frequency current transformer (RFCT) placed around a stator neutral cable conduit or the transformer neutral-earth connection. Unit shutdown is not required to place the RFCT. A transfer impedance of five ohms results in the frequency range of interest of 100 kHz to 100 MHz. The signals were captured at a sampling rate of 32kHz using an Agilent EMI device which follows the CISPR16 standard, Comité International Spécial des Perturbations Radioélectriques, filter designs for radio disturbance and immunity measuring apparatus. The identified conditions in these signals are PD and corona. The two signals were measured at 8.5MHz and 10.1MHz respectively on the Quasi peak detector.

Application

WATV and ALIF-TV parameters were fixed to $\mu = 1$ and $\eta = 0.95$. These values were chosen based on a grid search method for optimum performance. Both algorithms were applied to one PD signal, captured at the generator, and one Corona signal captured at the Generator Step-Up.

RESULTS

The performance of the methods was evaluated in terms of Mean Squared Error (MSE), as employed in [4], which is calculated as follows:

$$MSE = \frac{\sum_{i=0}^N [y(i) - \hat{x}(i)]^2}{N\sigma^2} \quad (18)$$

where $y(i)$ is the noisy EMI signal, $\hat{x}(i)$ is the denoised output of the algorithms and σ is the noise power. The calculated MSE for both algorithms is presented in Table (4). It is observed that ALIF-TV performs better than WATV in terms of MSE for both signals. A significant difference is seen in MSE of the denoised PD signal, however the performance on corona signal is almost similar. ALIF-TV output signals are illustrated in Figures 2 and 4 for PD and Corona signals respectively. Similarly, WATV output signals are illustrated in Figure 1 and 3. It is seen that noise was successfully reduced using both methods. Despite that Corona signal is extremely noisy, the algorithms performance was successful in that the shape of Corona discharges was extracted. It is also noticed that the WATV output signal is smoother than ALIF-TV. These results may facilitate the analysis of PD measurements for fault detection and classification between PD and Corona since the signals' shape has unique and clear pattern after denoising.

Table 4 Output MSE of the denoising methods

Signal	WATV	ALIF-TV
PD	0.3980	0.3678
Corona	0.3556	0.3517

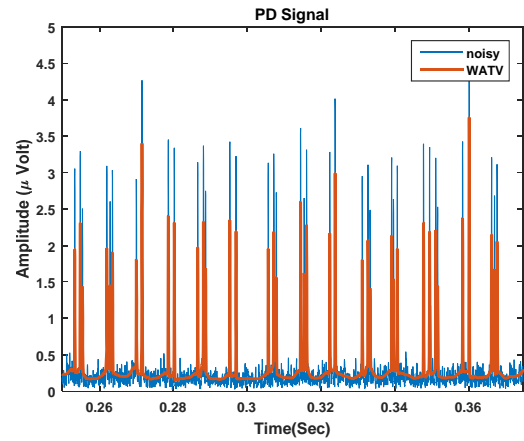


Figure 1 Noisy and denoised PD signal output of WATV algorithm

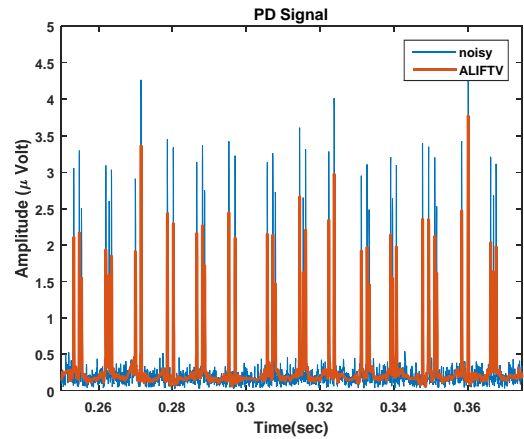


Figure 2 Noisy and denoised PD signal output of ALIF-TV algorithm

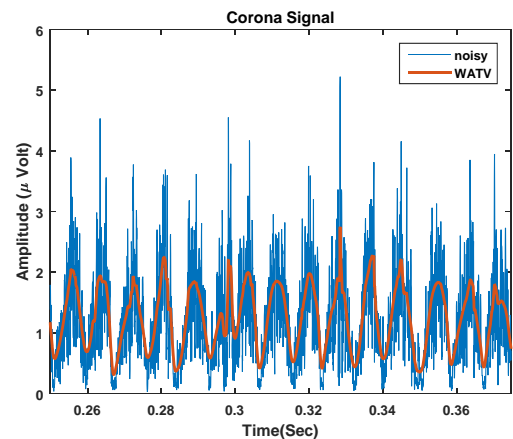


Figure 3 Noisy and denoised Corona signal output of WATV algorithm

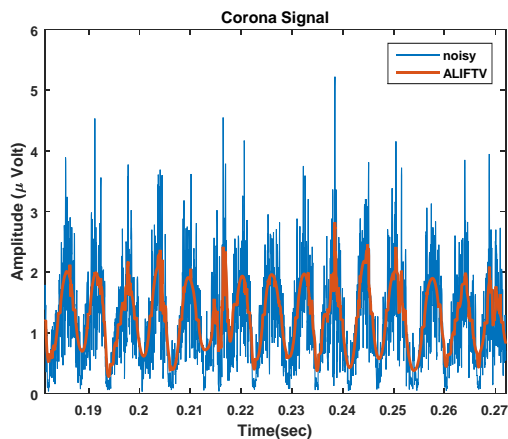


Figure 4 Noisy and denoised Corona signal output of ALIF-TV algorithm

CONCLUSION

In this paper we investigated the application of modern signal denoising techniques for non-stationary signals to real PD signals. We also introduced a new method ALIF-TV based on signal decomposition and TV, inspired by WATV developments. The methods' performance were evaluated and compared on the basis of their MSE metric. It was found that ALIF-TV outperforms WATV when applied to PD signals. Both algorithms were successful in reducing AWGN noise observed in our data. Other than AWGN, impulsive noise may also be an issue in PD field. However, it is not present in our data. This can be investigated as future work. The outcome of this paper can be exploited in condition monitoring for EMI fault diagnosis as pre-processing which will clean the signal to aid interpretation of PD information.

REFERENCES

- [1] *High Voltage Test Techniques- Partial Discharge Measurements*, (2000).
- [2] D. Evagorou, A. Kyprianou, P. L. Lewin, A. Stavrou, V. Efthymiou, and G. E. Georghiou, "Evaluation of Partial Discharge Denoising using the Wavelet Packets Transform as a Preprocessing Step for Classification," (2008).
- [3] J. Nelson, "Assessment of Partial Discharge and Electromagnetic Interference On-line Testing of Turbine-Driven Generator Stator Winding Insulation Systems," EPRI, Palo Alto, (2003).
- [4] S. Sriram, S. Nitin, K. Parabhu, and M. Bastiaans, "Signal Denoising Techniques for Partial Discharge Measurements," *IEEE Trans. Dielectr. Electr. Insul.*, 12, pp. 1182–1191, (2005).
- [5] H. D. Mota, L. D. Rocha, T. d. M. Salles, and F. Vasconcelos, "Partial Discharge Signal Denoising with Spatially Adaptive Wavelet Thresholding and Support Vector Machines,"

- Electr. Power Syst. Res.*, 81, , pp. 644–659, (2011).
- [6] T. Abdel-Galil, A. El-Hag, A. Gaouda, M. Salama, and R. Bartnikas, "De-noising of Partial Discharge Signal Using Eigen Decomposition Technique," *IEEE Trans. Dielectr. Electr. Insul.*, 15, pp. 1657–1662, (2008).
- [7] C. Cunha, A. Carvalho, M. Petraglia, and A. Lima, "A New Wavelet Selection Method for Partial Discharge Denoising," *Electr. Power Syst. Res.*, 125, pp. 184–195, (2015).
- [8] B. Vigneshwaran, R. Maheswari, and P. Subburaj, "An Improved Thresholding Estimation Technique for Partial Discharge Signal Denoising using Wavelet Transform", *ICCPCT Conference, Rio de Janeiro Brazil*, pp. 300–305, (2013).
- [9] X. Zhongrong, T. Ju, and S. Caixan, "Application of Complex Wavelet Transform to Suppress White Noise in GIS UHF PD Signals," *IEEE Trans. Power Deliv.*, 22, pp. 1498–1504, (2007).
- [10] J. Tang, Z. Xu, and C. Sun, "Investigation of Suppressing PD White Noise by Compound Information of Complex Wavelet Transform," *Eur. Trans. Electr.*, 19, pp. 313–322, (2009).
- [11] Y. Ding and I. W. Selesnick, "Artifact-Free Wavelet Denoising: Non-convex Sparse Regularization, Convex Optimization," *IEEE Signal Process. Lett.*, 22, pp. 1364–1368, (2015).
- [12] A. Cicone, J. Liu, and H. Zhou, "Adaptive local iterative filtering for signal decomposition and instantaneous frequency analysis," *Appl. Comput. Harmon. Anal.*, 41, pp. 384–411, (2016).
- [13] M. Afonso, J. Bioucas-Dias, and M. T. Figueiredo, "Fast Image Recovery Using Variable Splitting and Constrained Optimization," *IEEE Trans. Image Process.*, 19, pp. 2345–2356, (2010).
- [14] D. L. Donoho, "De-noising by soft-thresholding," *IEEE Trans. Inf. Theory*, 41, pp. 613–627, (1995).
- [15] N. E. Huang et al., "The Empirical Mode Decomposition and The Hilbert Spectrum for Nonlinear and Non-Stationary Time Series Analysis," *Proc. R. Soc. Lond. Math. Phys. Eng. Sci.*, 454, pp. 903–995, (1998).